Gold mineralization in the Cantung W-skarn deposit, Northwest Territories: An examination of distribution, mineralogy, and petrogenesis

E.M. Palmer[1], C.R.M. McFarlane[1], D.R. Lentz[1] and H. Falck[2]

1. University of New Brunswick, 2 Bailey Drive, Fredericton, New Brunswick
2. Northwest Territories Geoscience Office, PO Box 1320, Yellowknife, Northwest Territories

Abstract: The Cantung mine is a world-class W-skarn deposit; it is located just east of the Yukon border in the Selwyn Mountain Range of the Northwest Territories. The deposit area is within the southern extent of the polymetallic Tintina Gold Belt, which has many notable intrusion-related Au deposits. The extensive W skarns at Cantung were developed by hydrothermal fluids that, based on earlier research, were determined to be predominately supercritical magmatic brines with homogenization temperatures ranging from 270-500°C. Mineralization is composed of calcic exoskarn replacement of a clean limestone and lower grade replacements in a calc- silicate/chert unit; these occur in both the operating open pit and underground mine (the E Zone). The main sulphide identified petrographically is pyrrhotite, which is abundant in all skarn facies. Scheelite and chalcopyrite are dominant and there is locally abundant sphalerite. Native Bi exhibits textures indicative of forming later than the silicate assemblage in the paragenetic sequence, and it is decorated by bismuthinite, Bi tellurides, Ag tellurides, and Bi selenides. Tungsten and Cu are the main mine products, but the Au potential of the deposit merits further investigation.

This study characterized the distribution, mineralogy, and petrogenesis of Au mineralization by examining five skarn samples with bulk rock Au assay values >0.5 ppm taken from the E Zone. No free gold or electrum were identified petrographically or by SEM and FEG- SEM analyses. A positive correlation (Spearman's Rank, r') of Au with Bi (0.76), Ag (0.70), Fe (0.64), Cu (0.64), and Mo (0.60) was identified using the bulk rock geochemical data (n = 48). The strong correlation between Bi and Au is suggestive of a liquid bismuth collector mechanism for Au enrichment. However, LA ICP-MS analysis of native Bi and Bi alloys failed to reveal significant Au predicted by the liquid bismuth collector model. In contrast, the highest Au concentration was encountered in hessite (Ag_2Te) and other tellurides. Nano-inclusions within chalcopyrite and silicate minerals were also investigated using FEG-SEM for their Au content, but their composition consisted of native Bi. The decoration of native Bi by bismuthinite, Bi tellurides, Ag tellurides, and Bi selenides provides evidence for a late stage S-, Ag-, and Te-rich fluid. This fluid is thought to have remobilized the Au and deposited it as lattice bound invisible Au within the tellurides. This new data constrains Au exploration targets at Cantung to areas of altered skarn or where there is a presence of telluride minerals

Originally presented Fredericton 2014: Geological Association of Canada - Mineralogical Association of Canada Joint Annual Meeting, Special Session 3: Discovering the Next Generation of Porphyry Deposits: Advancements in Locating and Understanding Hidden Intrusion-related Mineralization. May 21, 2014.

Corresponding author: Emily Palmer (epalmer@unb.ca)

Palmer, E.M., McFarlane, C.R.M., Lentz, D.R., and Falck, H., 2015. Gold mineralization in the Cantung W-skarn deposit, Northwest Territories: An examination of distribution, mineralogy, and petrogenesis; *in* TGI 4 – Intrusion Related Mineralisation Project: New Vectors to Buried Porphyry-Style Mineralisation, (ed.) N. Rogers; Geological Survey of Canada, Open File 7843, p. 415-428.

Gold mineralization in the Cantung W-skarn deposit, NWT:

AN EXAMINATION OF DISTRIBUTION, MINERALOGY, AND PETROGENESIS

EMILY PALMER
BSC STUDENT AT THE
UNIVERSITY OF NEW BRUNSWICK

Regional geology

- Tintina Gold Province (TGP): precious & base metals
  - Spatially & genetically defined to Cretaceous plutons
- Tombstone-Tungsten Belt: felsic, sub-alkalic, reduced intrusions
- S- to I-type granitic plutons of the Selwyn plutonic suite

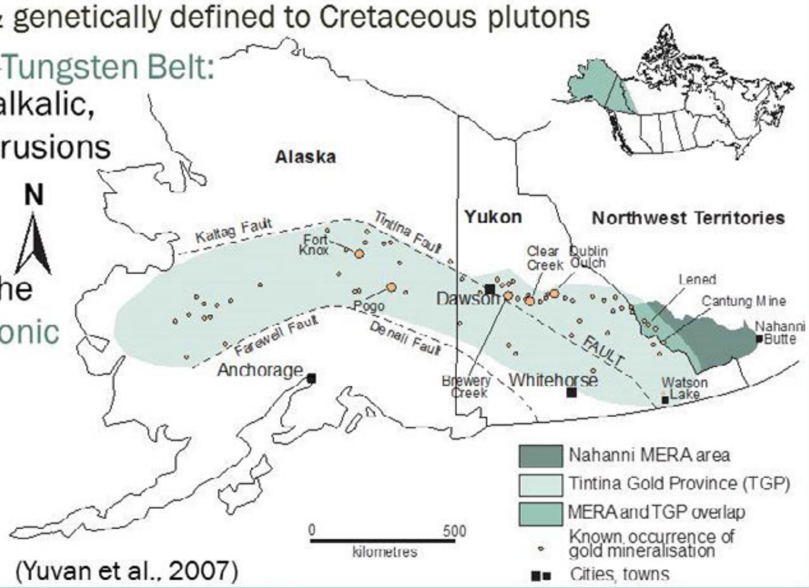

(Yuvan et al., 2007)

1

Local geology

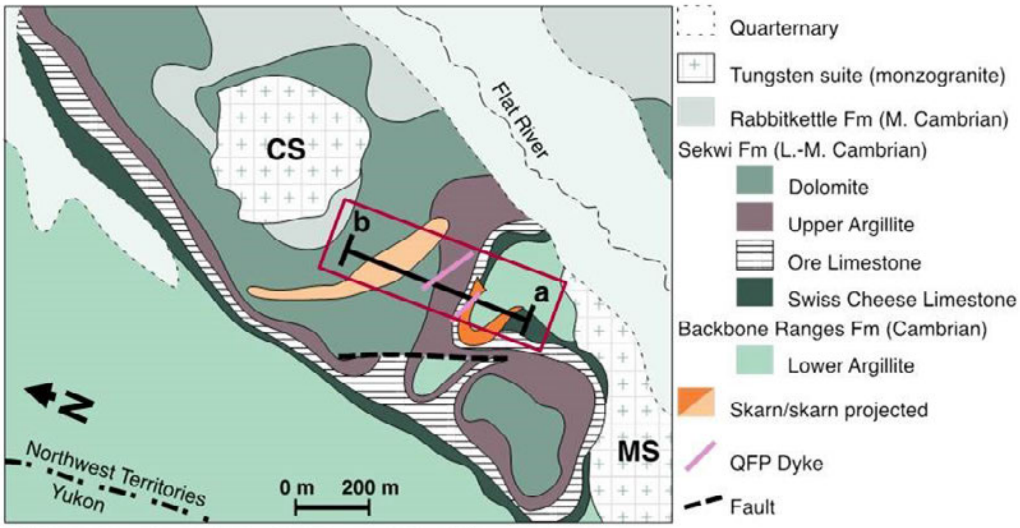

Surface geology at the Cantung mine. CS = circular stock. MS = mine stock (Rasmussen et al., 2011).

2

Local geology

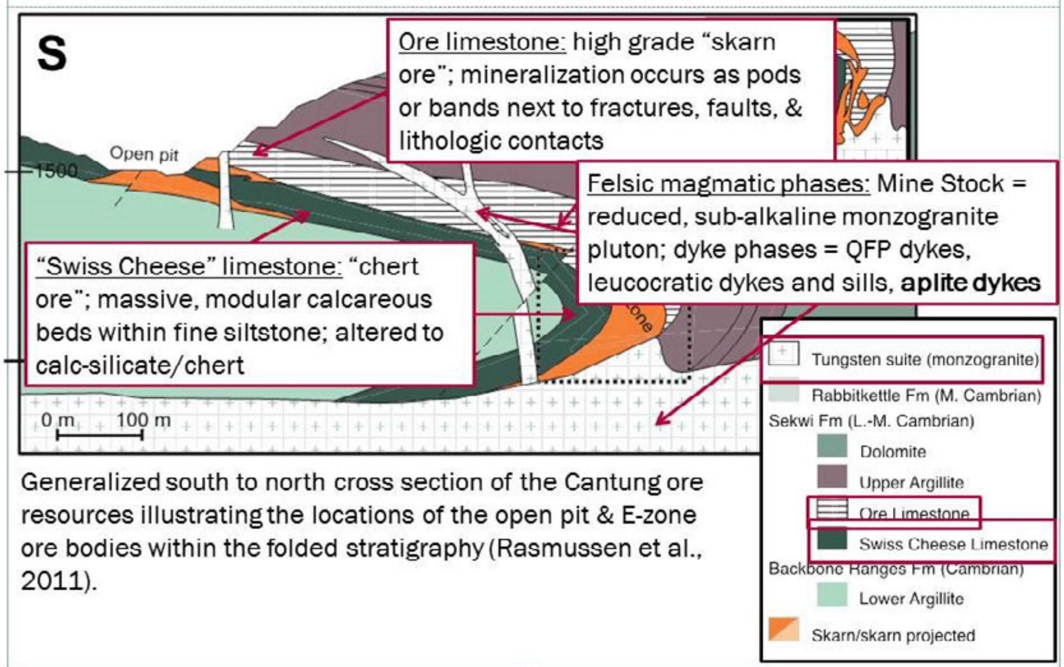

Generalized south to north cross section of the Cantung ore resources illustrating the locations of the open pit & E-zone ore bodies within the folded stratigraphy (Rasmussen et al., 2011).

3

Skarn formation

1. Prograde: contact metamorphism
   - Pluton intrudes country rock
   - Thermal maximum of 600°- 650°C (Mathieson and Clark, 1984)

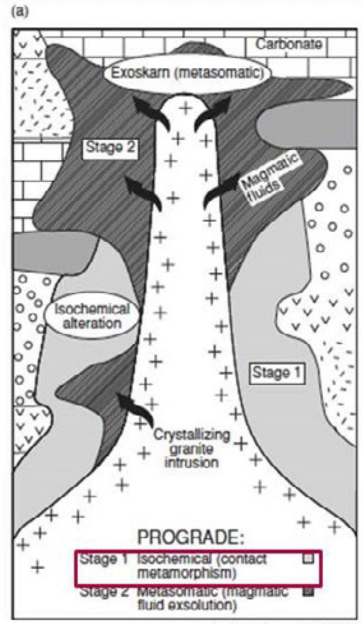

(Robb, 2005)

4

Skarn formation

2. Prograde: metasomatism
   - Magmatic fluid exsolution
     - Enrichment of H_2S, $FeCl_2$, $MgCl_2$, & KCl in main mineralizing fluid
     - Incompatible element enrichment in latest exsolved fluids
   - Egress of fluid phase into contact metamorphosed rock
   - Periodic trapping of fluid at crystallization front = over-pressuring
   - Pervasive metasomatism of aplite dykes (Rasmussen, 2011) = ongoing influx of magmatic fluid

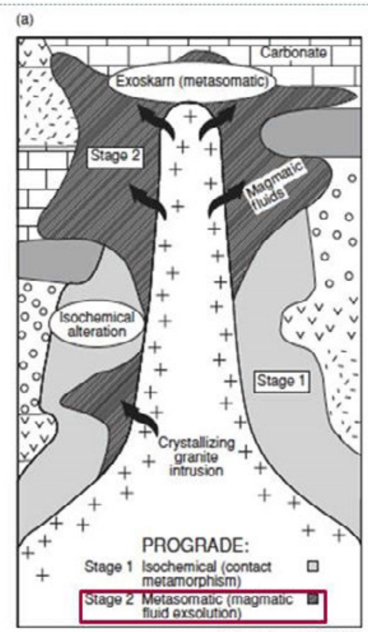

(Robb, 2005)

5

Skarn formation

3. Retrograde: meteoric fluid influx & main metal precipitation
   - Magmatic fluid neutralized by carbonates = increased pH
     - Enhances permeability & fluid flow
   - Decreased temperatures
   - Promotes precipitation of metals + sulphides
     - Pyrrhotite, scheelite, chalcopyrite, native Bi and Bi-minerals

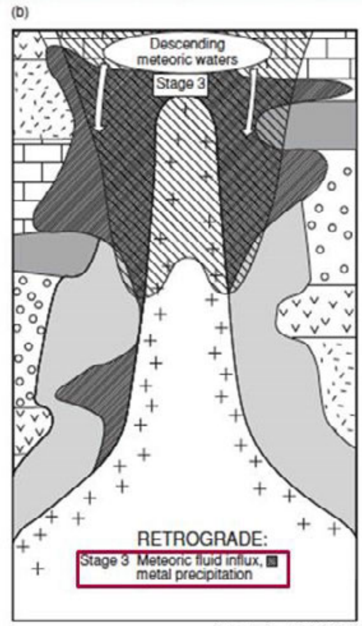

(Robb, 2005)

6

Objectives and purpose

- To characterize:
  - Distribution of Au
  - Petrogenesis of Au
  - Paragenetic sequence
- Purpose: are there economic concentrations of Au in the E-Zone?

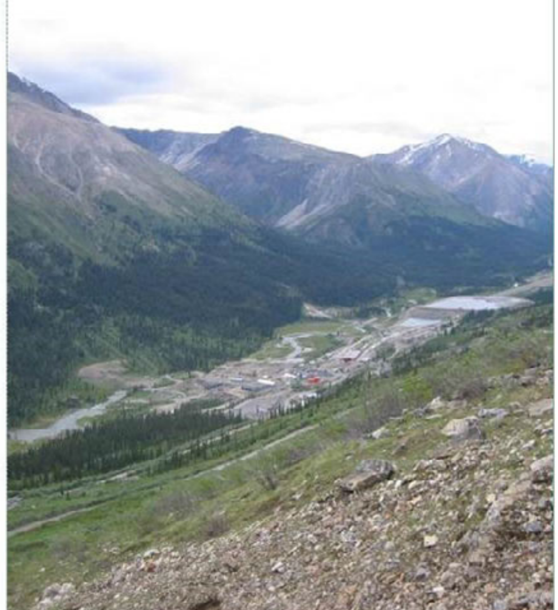

7

Analytical techniques

- Sample E-Zone
  - 46 samples
- Bulk rock geochemistry
  - Acid digestion, ICP-MS
- Petrography
  - Optical microscopy
  - SEM analysis
- FEG-SEM analysis
- LA ICP-MS analysis

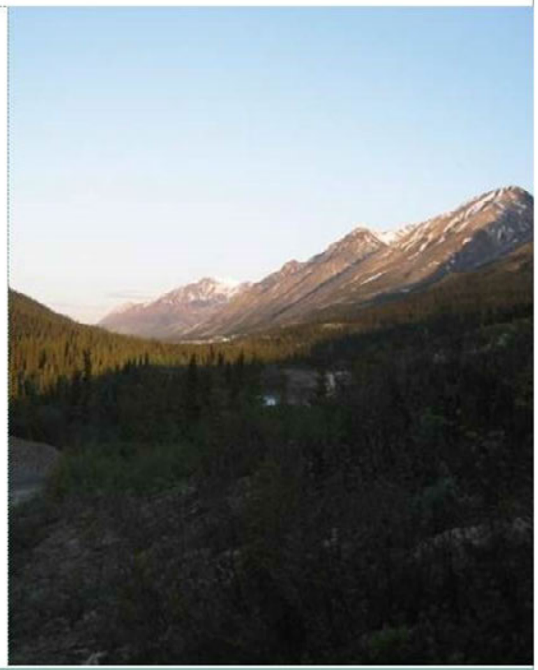

8

Geochemistry results

Sample #	03-DL-03	03-DL-04	03-DL-17a	03-DL-26	03-DL-27
Au (ppm)	0.9	0.6	0.9	1.3	8.0

- Spearman rank correlation coefficient
  - Measures statistical dependence of 2 variables
  - r' = +1: area rich in element 1 is likely to also have Au present
  - r' = -1: area rich in element 1 is likely to have no Au present
- Te and Se were not analyzed

9

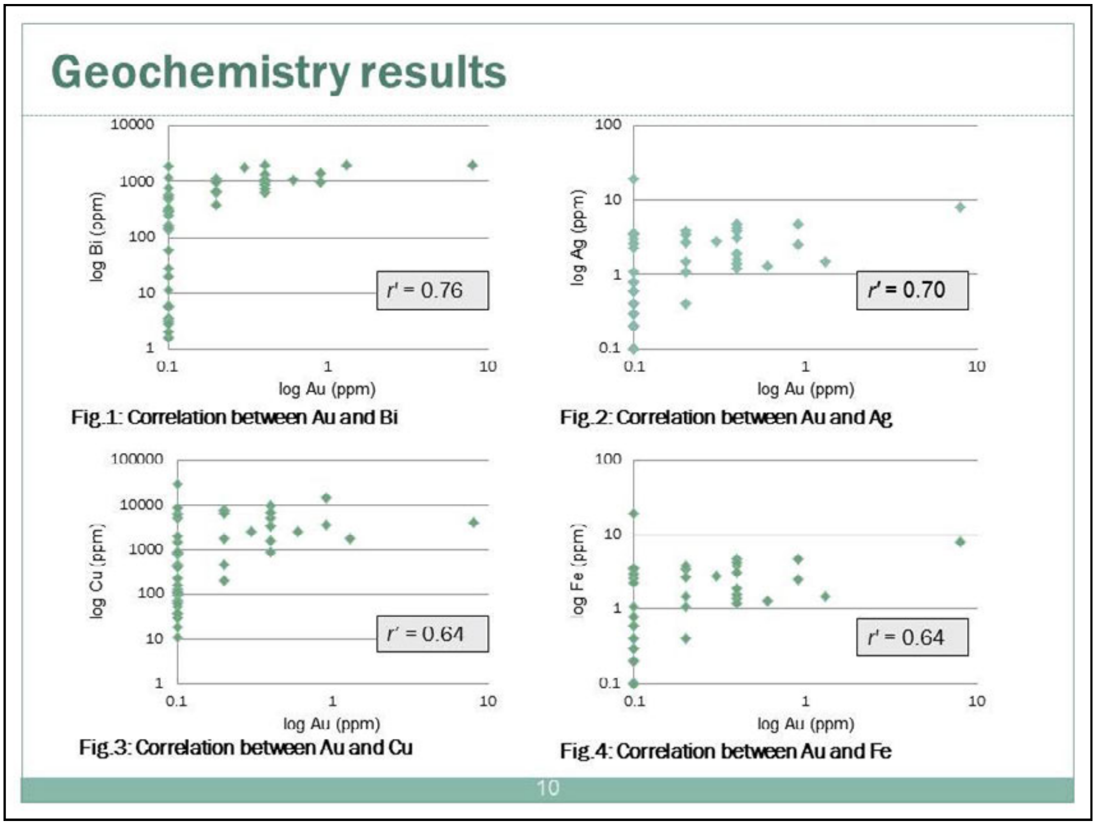
Geochemistry results
log Bi (ppm)
log Au (ppm)
r' = 0.76
Fig.1: Correlation between Au and Bi
log Ag (ppm)
log Au (ppm)
r' = 0.70
Fig.2: Correlation between Au and Ag
log Cu (ppm)
log Au (ppm)
r' = 0.64
Fig.3: Correlation between Au and Cu
log Fe (ppm)
log Au (ppm)
r' = 0.64
Fig.4: Correlation between Au and Fe
10

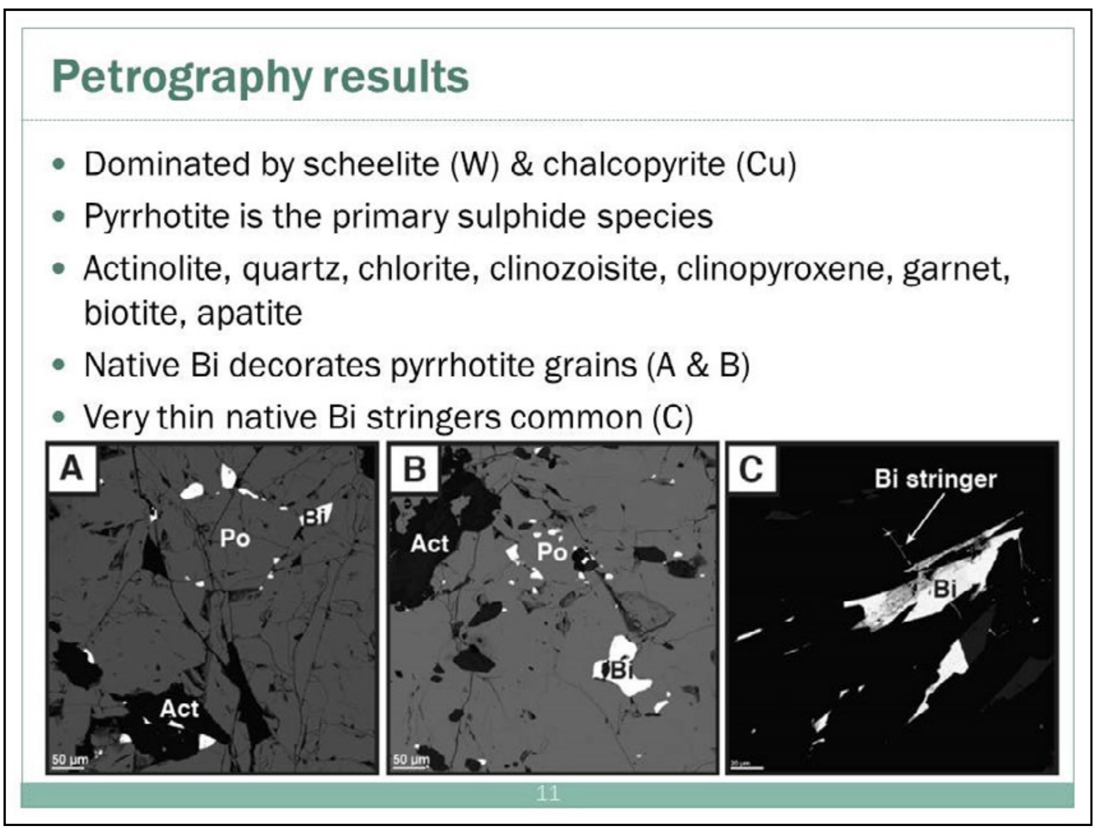
Petrography results
• Dominated by scheelite (W) & chalcopyrite (Cu)
• Pyrrhotite is the primary sulphide species
• Actinolite, quartz, chlorite, clinozoisite, clinopyroxene, garnet, biotite, apatite
• Native Bi decorates pyrrhotite grains (A & B)
• Very thin native Bi stringers common (C)
A
Po
Bi
Act
50 µm
B
Act
Po
Bi
50 µm
C
Bi stringer
Bi
11

Petrography results

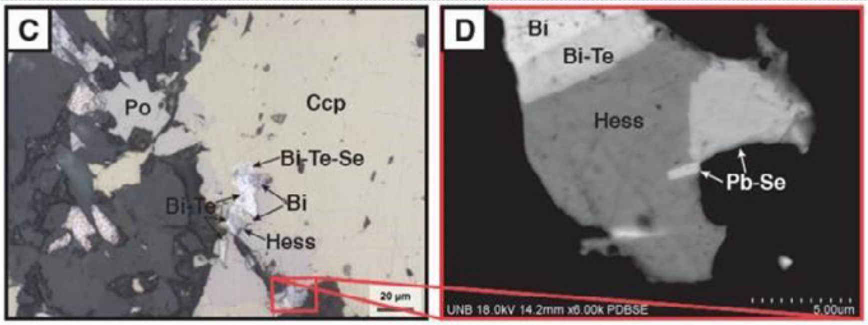

- Bi-sulfosalts, Bi-tellurides surround native Bi
- Native Bi & Bi-minerals found in association with zones of actinolite skarning
  - Hessite (Ag_2Te), Bi-tellurides, bismuthinite (Bi_2S_3) + sulfosalts
- No free Au present

12

FEG-SEM results

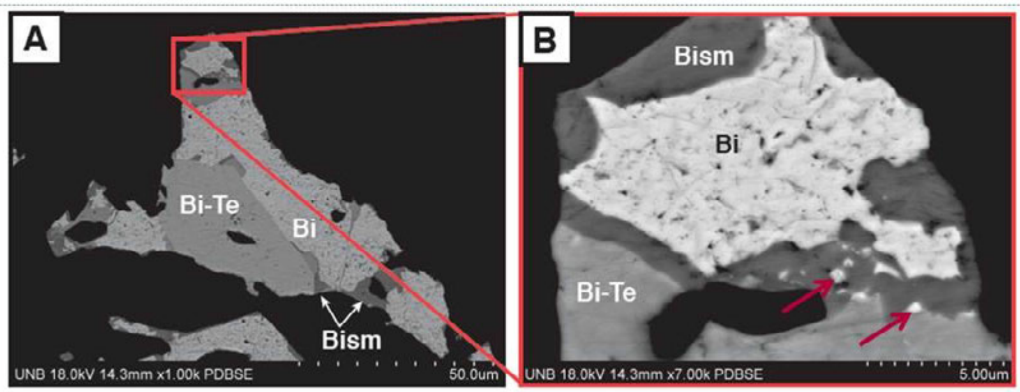

- Nano-inclusions in minerals, interstitial blebs, & stringers
  - Small (<1 µm), rounded to sub-rounded
- All that were analyzed = native Bi

13

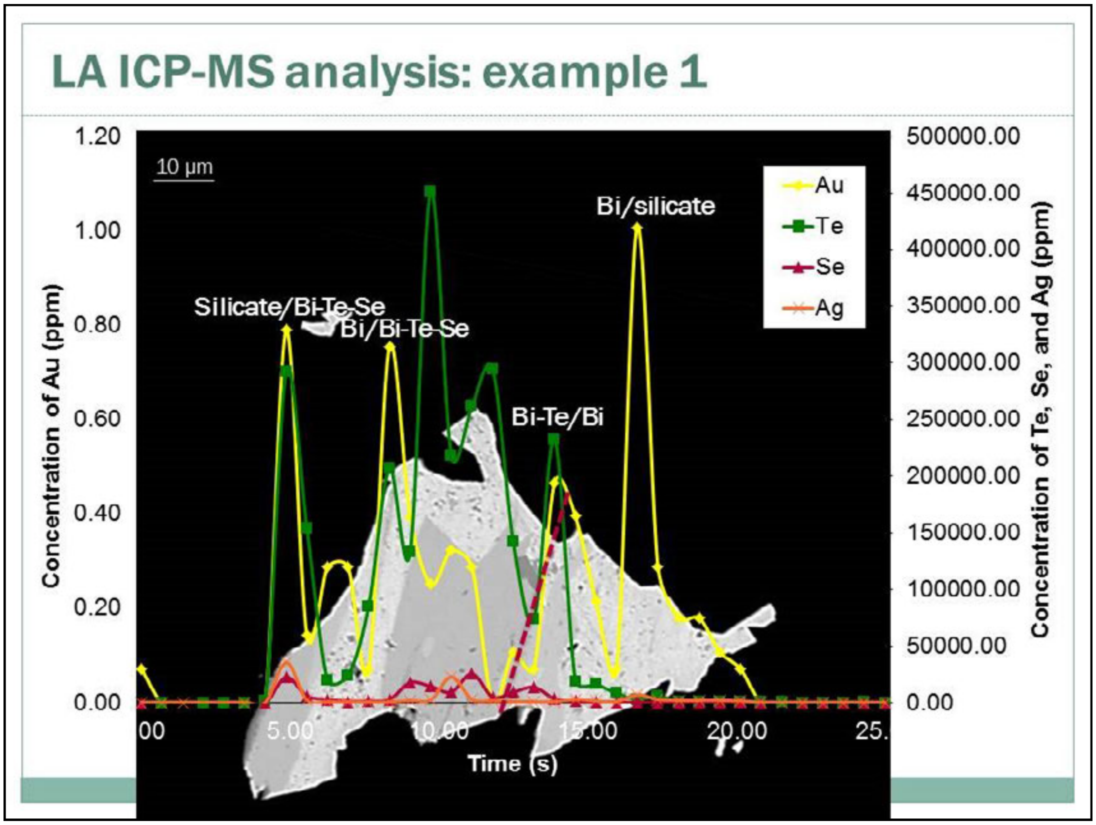
LA ICP-MS analysis: example 1
10 µm
Silicate/Bi-Te-Se
Bi/Bi-Te-Se
Bi-Te/Bi
Bi/silicate
Au
Te
Se
Ag
Concentration of Au (ppm)
Concentration of Te, Se, and Ag (ppm)
Time (s)

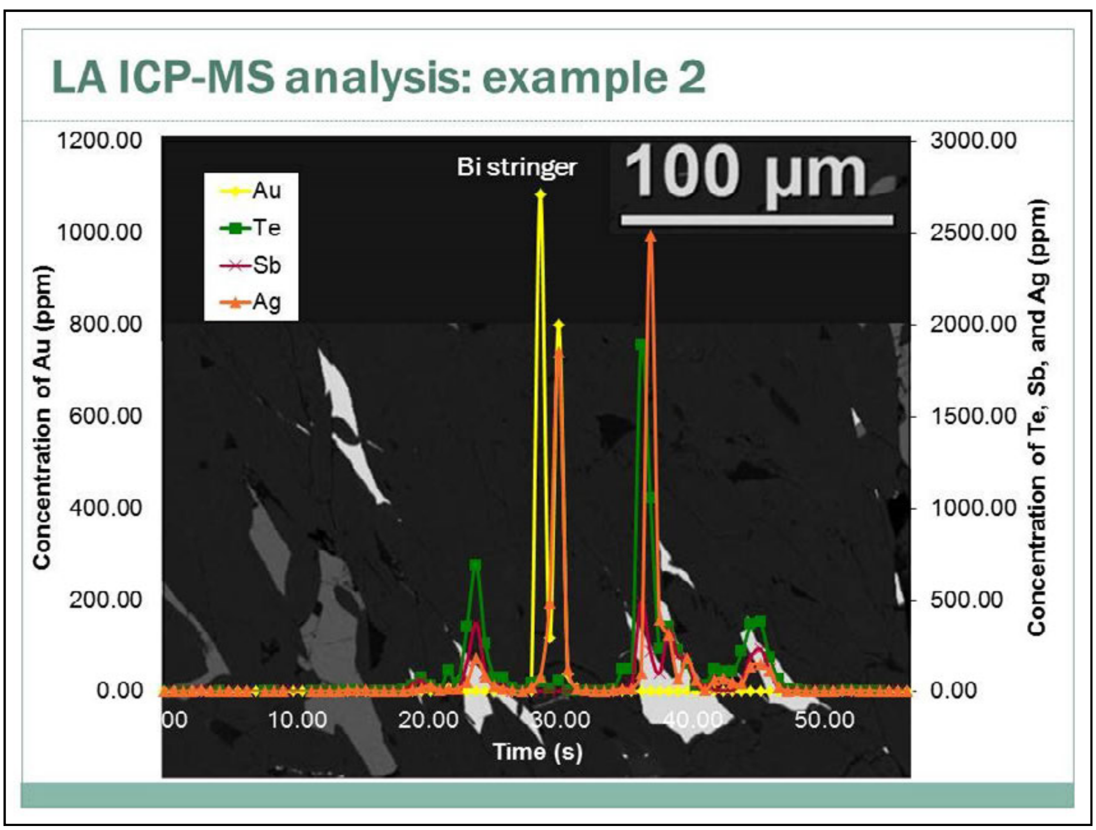
LA ICP-MS analysis: example 2
100 µm
Bi stringer
Au
Te
Sb
Ag
Concentration of Au (ppm)
Concentration of Te, Sb, and Ag (ppm)
Time (s)

Distribution of Au

- Au concentrated on outer rim of Bi-mineral grains
- 3 possibilities:

1. Solid solution as invisible Au within outer rim of Bi-minerals
2. Au nano-inclusions within/on edges of native Bi & Bi-minerals
3. Both lattice-bound & included as nano-inclusions

Au petrogenesis

- Au dissolves mainly as $AuCl^{-}_{2}$ at high temperatures
- Model A: high H_2S in fluid
- Solubility highest at high temperatures

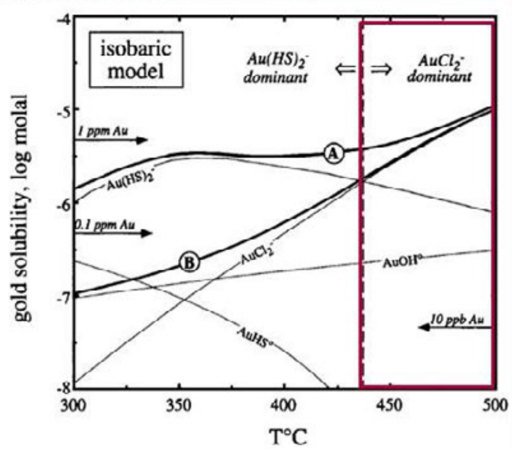

(Gammons and William-Jones, 1997)

17

Au petrogenesis

- Au dissolves mainly as $AuCl^{-}_{2}$ at high temperatures
- Model A: high H_2S in fluid
- Solubility highest at high temperatures
- Au precipitation:

1. Neutralization &/or
2. Reduction

- Likely remobilized by Cl^{-} complexes and later fluid deposited with Bi

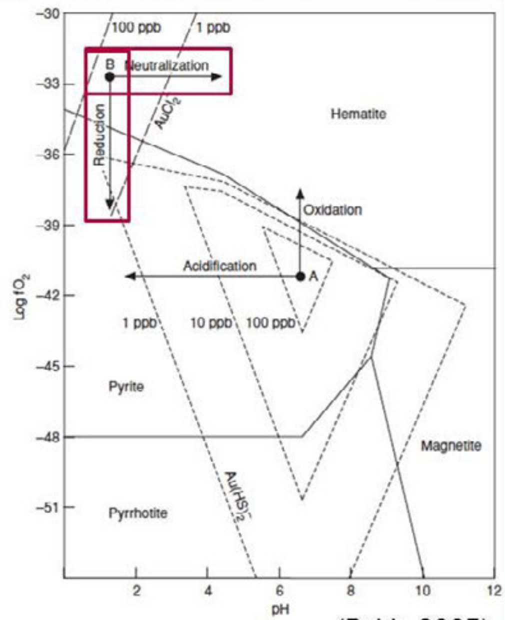

(Robb, 2005)

18

Au petrogenesis

- Liquid bismuth collector model: potential explanation for Au-Bi deposits (Douglas et al., 2000)
- Au partitions into Bi-melts even from undersaturated aqueous solutions (Tooth et al., 2008)

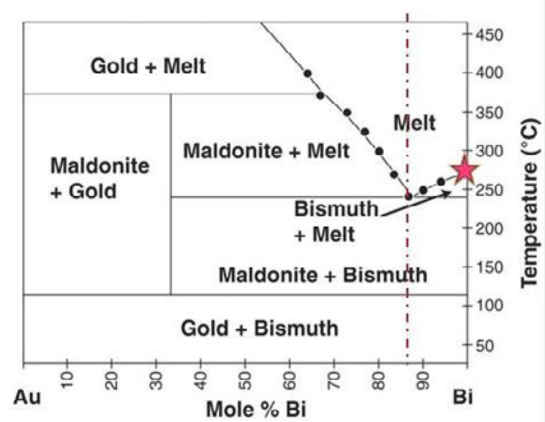

Phase diagram for Au-Bi system at 1 bar (Tooth et al., 2008). Native Bi has a melting temperature of 270ºC. Au-Bi melt has a eutectic with ~12 atomic % Au.

19

Au petrogenesis

- Likely aqueous Bi complex = $Bi(OH)_3$
  - Precipitation of Fe^{3+} minerals = reduction of Bi^{3+} to Bi^0 (melt)
- Alteration assemblages > 300°C (Mathieson and Clark, 1987)
  - Bi-Bi_2S_3 assemblage partially liquid for much of ore formation (270°C)
  - Liquid Bi reacting with skarn fluid system
- Crystallized at eutectic or lower Bi-Au-Ag-Pb-Te-Se-S eutectic (Cockerton and Tomkins, 2012)

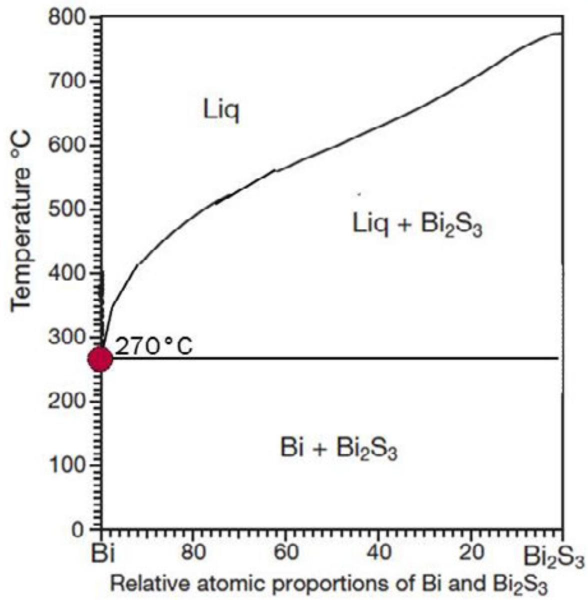

(Cockerton and Tomkins, 2012)

20

Conclusions

- No free Au present
  - Solid solution of Au on rims of Bi-minerals
  - Higher concentrations of Au likely occur as nanoparticles, although none identified
- Au transported from depth as $AuCl^{-}_2$
- Incorporated in Bi-minerals due to high affinity of Bi and Au
- Area at margin of reaction front more promising for Au exploration where massive sulphides are located
  - Fluid movement and remobilization constant within front until cooled

22

Paragenetic sequence

- Contact metamorphism:
  - Garnet, clinopyroxene
- Silication:
  - Actinolite, epidote, biotite, apatite, chlorite
- Main mineral precipitation:
  - Pyrrhotite, chalcopyrite, scheelite, sphalerite
  - Native Bi, bismuthinite, Bi-tellurides/Bi-Te-Se sulfosalts, hessite
  - Gold

21

Acknowledgements

I would like to thank Chris McFarlane and Dave Lentz for their direction and advice on the direction of the project; Douglas Hall and Steven Cogswell for their helpful expertise using the SEM; and Suporn Boonsue for her time and laughter while on the FEG-SEM.

Funding for this project was provided by the Northwest Territories Geoscience Office (NTGO). A special thank you to Hendrik Falck for pushing my opportunity to visit the NWT for a poster presentation on this project.

23

References

Cockerton, A.B.D., and Tomkins, A.G. (2012). Insights into the liquid bismuth collector model through analysis of the Bi-Au Stormont Skarn Prospect, Northwest Tasmania. *Economic Geology, 107*(4), 667-682.

Ciobanu, C. L., Birch, W. D., Cook, N. J., Pring, A., and Grundler, P. V. (2010). Petrogenetic significance of Au–Bi–Te–S associations: The example of Maldon, Central Victorian gold province, Australia. *Lithos, 116*(1-2), 1–17.

Ciobanu, C. L., Cook, N. J., and Pring, A. (2006). Bismuth tellurides as gold scavengers. *Mineralogy and Petrology, 87*(3-4), 277–304.

Ciobanu, C. L., Cook, N. J., Pring, A., Brugger, J., Danyushevsky, L. V., and Shimizu, M. (2009)."Invisible gold" in bismuth chalcogenides. *Geochimica et Cosmochimica Acta, 73*(7), 1970–1999.

Cook, N. J. and Ciobanu, C. L. (2004). Bismuth tellurides and sulphosalts from the Larga hydrothermal system, Metaliferi Mts, Romania: Paragenesis and genetic significance. *Mineralogical Magazine, 68*(2), 301–321.

Douglas, N., Mavrogenes, J., Hack, A., and England, R. (2000. The liquid bismuth collector model: an alternative gold deposition mechanism [abs.], in Silbeck, G., and Hubble, T.C.T., eds., Understanding planet Earth; searching for a sustainable future; on the starting blocks of the third millennium: 15th Australian Geological Convention Abstracts: Sydney, Geological Society of Australia, p. 135.

Mathieson, G. and Clark, A. (1984). The Cantung E Zone scheelite skarn orebody, Tungsten, Northwest Territories: a revised genetic model. *Economic Geology, 79*, 883–901.

Rasmussen, K. L., Lentz, D. R., Falck, H., and Pattison, D. R. M. (2011). Felsic magmatic phases and the role of late-stage aplitic dykes in the formation of the world-class Cantung Tungsten skarn deposit, Northwest Territories, Canada. *Ore Geology Reviews, 41*(1), 75–111.

Rasmussen, K. L. and Mortensen, J. K. (2013). Magmatic petrogenesis and the evolution of (F:Cl:OH) fluid composition in barren and tungsten skarn-associated plutons using apatite and biotite compositions: Case studies from the northern Canadian Cordillera. *Ore Geology Reviews, 50*, 118–142.

Tooth, B., Brugger, J., Ciobanu, C., and Liu, W. (2008). Modeling of gold scavenging by bismuth melts coexisting with hydrothermal fluids. *Geology, 36*(10), 815.

Yuvan, J., Shelton, K., Falck, H., 2007. Geochemical investigations of the high-grade quartz–scheelite veins of the Cantung Mine, Northwest Territories. In: Wright, D.F., Lemkow, D., Harris, J.R. (Eds.), Mineral and Energy Resource Assessment of the Greater Nahanni Ecosystem under Consideration for the Expansion of the Nahanni National Park Reserve, Northwest Territories. Geological Survey of Canada Open File 5344, pp. 177–190.